

## Feasibility study of GPS time series analysis with time-dependent periodic coefficients model (TDPC)

Arash Nazari<sup>1\*</sup>, Khosro Moghtased-Azar<sup>2</sup>

<sup>1</sup> Geodesy Department, Faculty of Civil Engineering, Tabriz University, Tabriz, Iran

<sup>2</sup> Assistant Professor at Department of Geomatics Engineering, Faculty of Civil Engineering, Tabriz University, 29 Bahman Boulevard, Tabriz, Iran

### Article history:

Received: 18 May 2020, Received in revised form: 28 January 2021, Accepted: 15 February 2021

ABSTRACT	KEYWORDS
<p>A time dependent periodic coefficients (TDPC) model was proposed to analyze the Global Positioning System (GPS) time series. Due to the variations of the amplitude and phase lag of the GPS signals over time, we propose a TDPC to analyze the daily time series. A new solution approach, where the serial correlations of the disturbances are eliminated by sequentially differencing the measurements, was used to estimate the model parameters using weighted least squares. As a numerical performance of the proposed method, the time series of 19 permanent stations in the United States via the Website of Scripps Orbit and Permanent Array Center (SOPAC) between the 2000 and 2010 year was selected. The results show a decrease in the RMS values of the residuals, especially for the height components. Moreover, using the 90 simulated GPS data analysis, in which their noises were different combinations of white noise and flicker noise, we demonstrate that the proposed model can extract amplitude varying periodic variabilities from GPS coordinate time series.</p>	<p>GPS Time series Least Squares Time-dependent Root Mean Square</p>

### 1. Introduction

The study of GPS time series in the past few years has demonstrated its support in monitoring the crustal movement. In addition, GPS position time series are used to study geophysical phenomena, including plate tectonics (e.g., Tobita., 2016), post-glacial rebound (e.g., Larson and van Dam., 2000), and vertical motions (e.g., Teferle et al., 2009). In all these cases, one normally estimates a secular motion or velocity with seasonal signals (Klos et al., 2018). Conventionally these signals are derived by least-squares fitting of harmonic terms with a constant amplitude and phase. In reality, their values might vary slightly from year

to year because their geophysical causes are not constant (Klos et al., 2018).

Accordingly, noise or so called residuals are created when the deterministic model was removed. For the GPS position time series, the power spectrum of the noise follows a power-law behavior at the low frequencies with spectral indices varying between -2 and 0. This noise significantly impacts the uncertainty of velocity (e.g., Zhang et al., 1997; Williams et al., 2004; Bogusz and Kontny., 2011). Moreover, suppose any seasonal signal or residual or periodicity is not properly modeled and removed. In that case, it will be moved to a stochastic part to much more

\* Corresponding author

E-mail addresses: [arash\\_nazari96@ms.tabrizu.ac.ir](mailto:arash_nazari96@ms.tabrizu.ac.ir) (A. Nazari); [moghtased@tabrizu.ac.ir](mailto:moghtased@tabrizu.ac.ir) (K. Moghtased-Azar)

DOI: 10.22059/eoge.2021.325586.1097

correlated noise, causing the uncertainties to be artificially overestimated (e.g., [Tehranchi et al., 2020](#)).

Several studies have suggested determining the time-varying periodic signals by relying, for instance, on non-parametric annual signals (e.g., [Freymuller., 2009](#); [Tesmer et al., 2009](#)), on Kalman filter based technics (e.g., [Murray and Segall., 2005](#), [Davis et al., 2012](#)), singular spectrum analysis (SSA) to model time-varying signals in weekly GPS position time series (e.g., [Chen., 2013](#)), piecewise continues linear polynomials (e.g., [Davis et al., 2006](#)).

In this paper, we introduce a TDPC model and assess the ability of this model to obtain variations of time-varying seasonal signals. In the proposed model, the periodic terms of the functional model change linearly over time. Unlike the conventional method, the seasonal effects do not have a fixed amplitude and are time-dependent. After modeling and eliminating the systematic impact of the functional model (seasonal signals and trends as well as identifying and detecting outliers and offsets), we assess the statistical characteristics of the residuals. The statistical model based on the first-order autoregressive process is introduced, and a differencing algorithm is used to reduce the correlation of disturbances. Based on this, the noise properties of the time series are investigated.

In the following, we briefly describe the conventional method (constant amplitude model) of GPS time series analysis and estimate model parameters using the weighted least squares. Afterward, we introduce the statistical model and noise characteristics in the GPS time series. In Section 3, the TDPC model and its features are introduced in detail. As the numerical results, the time series of nineteen stations spanning ten years of SOPAC daily coordinate positions between 2000 and 2010 are analyzed by both methods. The ability of the proposed model in modeling the GPS signals, compared to the conventional method (least squares) using root mean squares (RMS). The last section drafts several conclusions.

## 2. Conventional functional model in GPS time series analysis

The functional model of GPS time series generally is defined as follows:

$$y_t = y_0 + vt + \sum_{k=1}^q (a_k \sin(\omega t) + b_k \cos(\omega t)) + e_t \quad (1)$$

where  $y_t$  is the observation vector,  $y_0$  is the intercept,  $v$  is a constant velocity,  $a_k$  and  $b_k$  are the coefficients of periodic terms, and  $e_t$  is the noise term. In the case of a linear trend together with annual and semi-annual signals ( $q=2$ ), the  $i$ th row of design matrix becomes:

$$A = [1 \quad t_i \quad \sin(2\pi t_i) \quad \cos(2\pi t_i) \quad \sin(4\pi t_i) \quad \cos(4\pi t_i)] \quad (2)$$

and the unknowns vector  $x$  is:

$$x = [y_0 \quad v \quad a_1 \quad b_1 \quad a_2 \quad b_2]^T \quad (3)$$

so that:

$$y = Ax + e \quad (4)$$

If the covariance matrix of the observation  $Q_y$  is known, the least-squares solution for unknown parameters is:

$$\hat{x} = (A^T W A)^{-1} A^T W y \quad (5)$$

where  $W$  is the weighted matrix and is defined as  $W = Q_y^{-1}$ , and finally the estimated residuals:

$$\hat{e} = y - A\hat{x} \quad (6)$$

For the case of uncorrelated white noise, the observation covariance matrix is defined by the individual measurement variances,  $\sigma_i^2$ :

$$Q_y = \begin{bmatrix} \sigma_1^2 & 0 & 0 & \cdots & 0 \\ 0 & \sigma_2^2 & 0 & \cdots & 0 \\ 0 & 0 & \sigma_3^2 & \cdots & 0 \\ \vdots & \vdots & \vdots & \ddots & \vdots \\ 0 & 0 & 0 & \cdots & \sigma_N^2 \end{bmatrix} \quad (7)$$

### 2.1 Spectrum analysis

The power spectrum  $p_y$  of many geophysical phenomena, including the noise in GPS position time series, is well approximated by a power-law process ([Mandelbort, 1983](#), [Mao et al., 1999](#); [Williams, 2003](#); [Williams et al., 2004](#)). The one-dimensional time behavior of the stochastic process is such that its power spectrum has the form:

$$p_y(f) = p_0 \left( \frac{f}{f_0} \right)^k \quad (8)$$

where  $f$  is the temporal frequency,  $p_0$  and  $f_0$  are the normalizing constants, and  $k$  is the spectral index (see, e.g., [Mandelbrot and van Nes., 1968](#)). Typical spectral index values lie within  $[-3,1]$ ; for stationary process  $-1 < k < 1$  and for non-stationary process  $-3 < k < -1$ . Classical white noise has a spectral index of 0, flicker noise has a -1, and random walk noise has a spectral index of -2. The power spectral method can be employed to assess the noise characteristic of GPS time series.

### 2.2 Stochastic model

To describe the characteristic of colored noise, several models are adopted, for instance, the power-law noise model ([Zhang et al., 1997](#); [Williams et al., 2004](#)) and the first-order Gauss-Markov (FOGM) model ([Langbein, 2004](#)). If the time series of GPS coordinates is composed of white noise and flicker noise, with variance  $\sigma_w^2$  and  $\sigma_f^2$  respectively, the covariance matrix of the time series can then be written as:

$$Q_y = \sigma_w^2 I + \sigma_f^2 Q_f \quad (9)$$

where  $I$  is the  $m \times m$  identity matrix and  $Q_f$  is the cofactor matrix of flicker noise. The structure of  $Q_y$  is known

through  $I$  and  $Q_f$ , but the contributions through  $\sigma_w$  and  $\sigma_f$ , are unknown (Amiri-Simkooei et al., 2007). The elements of the flicker noise cofactor matrix  $Q_f$  can be approximated by (Zhang et al., 1997):

$$q_{ij}^{(f)} = \begin{cases} \frac{9}{8} & \text{if } \tau = 0 \\ \frac{9}{8} \left(1 - \frac{\log \tau / \log 2 + 2}{24}\right) & \text{if } \tau \neq 0 \end{cases} \quad (10)$$

where,  $\tau = |t_j - t_i|$ . For evenly spaced data, the matrix  $Q_f$  is a symmetric Toeplitz matrix that contains values along negative-sloping diagonals. It is important to note that the Hosking flicker noise covariance matrix, which was introduced and used by Williams [2003], can also be used. The variance components  $\sigma_w^2$  and  $\sigma_f^2$  can now be estimated using the Least Squares Variance Component Estimation (LS-VCE) method. The main advantage of the least-squares is its ease of implementation and the straightforward interpretation of the estimates of a linear trend and seasonal signal amplitudes. Nevertheless, only constant amplitude and phases are obtained. One disadvantage of the technique is that long-periodic variations can be mistakenly identified as a linear trend (Rangelova et al., 2012). However, this problem not be an issue here as we will be estimating annual and semi-annual signals from multi-year time series (Bellewit and Lavell., 2002).

### 3. Time-dependent periodic coefficient model (TDPC)

In this section, we introduce the TDPC and assess the ability of this model to obtain changes in these signals.

#### 3.1 Functional model

The functional model of GPS positions time series, with a TDPC (state of time-dependent amplitude model), is as follow:

$$y_t = a + b(t - \bar{t}) + \sum_{i=1}^m \alpha(t)_i \sin\left(\frac{2\pi}{p_i}(t - \bar{t})\right) + \sum_{i=1}^m \beta(t)_i \cos\left(\frac{2\pi}{p_i}(t - \bar{t})\right) + e_t \quad (11)$$

$t = 1, \dots, T$

where in this expression,  $y_t$  is the observation at a given epoch  $t$ , and  $\bar{t}$  refers to the middle of the series. The parameter  $a$  is the intercept of a trend with slope  $b$  that represents the secular variations in the GPS components to be estimated,  $p$  represents the periods of seasonal signals (annual and semi-annual signals),  $T$  is also the total length of the time series. The disturbances,  $e_t$ , (measurements errors) are assumed to be uncorrelated, stationary, and either homogeneous or heterogeneous for both representations.

$\alpha(t)$  and  $\beta(t)$  are the time-varying coefficients that vary linearly in time. The linear rates of changes in the harmonic coefficients, denoted by  $\dot{\alpha}$  and  $\dot{\beta}$ , are introduced together with their corresponding intercepts as an additional unknown parameter to be estimated as follow:

$$\alpha(t)_i = \alpha_i^0 + \dot{\alpha}_i(t - \bar{t}) \quad (12)$$

$$\beta(t)_i = \beta_i^0 + \dot{\beta}_i(t - \bar{t}) \quad (13)$$

where,  $\alpha_i^0$  and  $\beta_i^0$  are the nominal values of the harmonic coefficients (intercepts of the trends). Total amplitude is defined as follow:

$$A = \sqrt{\alpha(t)_i^2 + \beta(t)_i^2} \quad (14)$$

#### 3.2 Statistical model

The daily positions of permanent GPS stations are usually considered randomly independent of each other. Meanwhile, errors such as modeling satellite orbits, determining rotational parameters, atmospheric modeling parameters, etc., cause correlations between daily positions or color noise between daily positions of stations. A differencing algorithm (Iz and Chen., 2001) is used to reduce this serial correlation, which will be described below, which leads to the absorption of part of the colored noise in the estimation of seasonal signals. The statistical model for the model disturbances is considered to be an autoregressive process, which is represented as a first-order process in this study as follow:

$$e_t = \rho e_{t-1} + v_t \quad (15)$$

where this expression,  $\rho$  is the first-order autocorrelation coefficient,  $\{v_t\}$  is the stochastic process with the following assumed properties (Iz, 2008):

$$E(v_t) = 0, E(v_t^2) = \sigma_v^2, E(v_t v_{t'}) = 0, \text{ for } t \neq t' \quad (16)$$

$$\Rightarrow E(e_t) = 0, E(e_t^2) = \sigma_v^2(1 - \rho^2) = \sigma^2$$

where  $E$  is the mathematical expectation operator. It can be shown that the corresponding covariance matrix for the model disturbances can now be expressed as (Iz and Chen., 1999):

$$\Sigma = \sigma^2 \begin{bmatrix} 1 & \rho & \rho^2 & \dots & \rho^{T-1} \\ \rho & 1 & \rho & \dots & \rho^{T-2} \\ \vdots & \vdots & 1 & \dots & \vdots \\ \rho^{T-1} & \rho^{T-2} & \dots & 1 & \end{bmatrix} \quad (17)$$

A two-stage approach can obtain the solution for the time variable harmonic coefficients with its statistical model.

First stage: the correlation coefficients are estimated from the residuals of an approximation (according to the initial periods). The second stage: use the above covariance matrix. The mentioned solution has two main problems: (i) A significant assumption in this approach is that the stochastic process is stationary and the corresponding disturbances are homogeneous (that this assumption is not valid), (ii)- Furthermore, although the above statistical model accounts for the effect of serial correlation, it fails to model the weights (Iz, 2008) properly. Due to the mentioned problems, we use a differencing algorithm as follow:

### 3.3. Model transformation via differencing

The model given by (11) is rewritten as

$$y_t = x_0 + a_{1t}x_1 + a_{21t}x_2 + \dots + a_{1t}x_{kt} + e_t \quad (18)$$

where,  $x$  denotes the parameters to be estimated, and  $a$ 's are the corresponding known coefficients. Differencing model is defined as follow: If the model (18) is evaluated at the preceding epoch,  $t - 1$ , and multiplied by  $\rho$  (estimated from approximate solution residuals), and then subtracted from itself which is evaluated at  $t$  as shown in (19), then:

$$\Delta y_t = (1 - \rho)x_0 + \Delta a_{1t}x_1 + \Delta a_{21t}x_2 + \dots + \Delta a_{1t}x_{kt} + v_t \quad (19)$$

where:

$$\begin{aligned} \Delta y_t &= y_t - \rho y_{t-1} \\ \Delta a_t &= a_t - \rho a_{t-1} \\ v_t &= e_t - \rho e_{t-1} \end{aligned} \quad (20)$$

Observe that the differencing leave the unknown parameters  $x_k$  invariant; therefore, the transformed observation Eq. (19) can be solved using an LS solution with a diagonal covariance matrix of the stochastic process  $\{v_t\}$  which is given by:

$$\Sigma = \sigma^2 \begin{bmatrix} v_1 & 0 & 0 & \dots & 0 \\ 0 & v_2 & 0 & \dots & 0 \\ \vdots & \dots & \dots & \dots & \vdots \\ 0 & 0 & 0 & \dots & v_T \end{bmatrix} \quad (21)$$

If the correction coefficient is high (near to one), then the following approximations can be made:

$$\begin{aligned} \Delta y_t &= y_t - \rho y_{t-1} \cong y_t - y_{t-1} \\ \Delta a_t &= a_t - \rho a_{t-1} \cong a_t - a_{t-1} \end{aligned} \quad (22)$$

and (19) reduces to:

$$\Delta y_t = \Delta a_{1t}x_1 + \Delta a_{21t}x_2 + \dots + \Delta a_{1t}x_{kt} + v_t \quad (23)$$

This approximation is reasonable, especially for the daily GPS time series. If all systematic variations in the series are properly accounted for, then the residuals reflect the accuracy of the measurements, i.e., the RMS solution residuals should be close to a reported sub-mas measurement precision of modern satellite-born techniques.

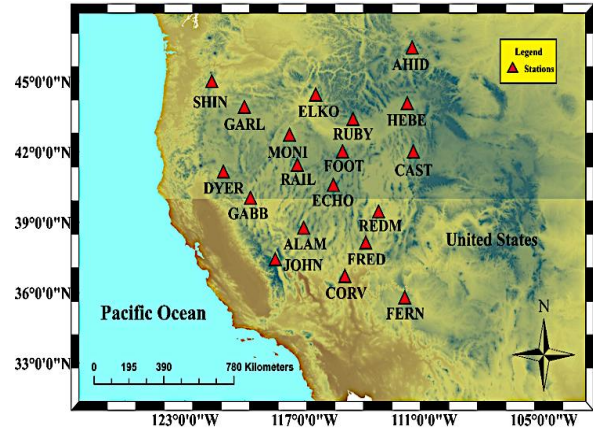


Figure 1. Distribution of the stations used in this study.

### 4. Numerical examples

This section presents the results of the coordinate time series analysis using the methodology explained in previous sections. Figure. 1 shows the distribution of selected stations used in this research. The time series of 19 stations in the Western United States were selected from the 2000 and 2010 years.

The daily positions of the network are processed by the SOPAC processing center using GAMIT-GLOBK software, and the result is placed in the ITRF2000 reference framework on the center's website. It is important to note that outliers have been removed from the coordinates time series of each station by the median and Inter Quartile Range (IQR) statistics. Also, offset epochs are detected and removed from the data.

The solution requires a set of periods for the presumably known frequencies. The periods used in the solution are 365.24 for the annual periodic signal, 182.4 for the semi-annual periodic signal, and 350/n of significant periodic patterns with periods of 350 days and its fractions 350/n,  $n = 2, \dots, 8$ .

Figure 2 displays the comparisons of fitting two methods (LS and TDPC) in three components of the ALAM station (left panel) and ELKO station (right panel) of selected permanent stations. It is clearly shown that the amplitude of the time series and true seasonal variation is not constant from year to year. The LS-derived curve generally fits the time series well while failing to capture the peak from time to time. However, as seen from the figure, the TDPC model has modeled the amplitude variation in time series. As we expect, the difference between the models is more visible due to the higher amplitudes of noise

components over the vertical component.

and lower quartiles, hence the terms box-and-whisker plot

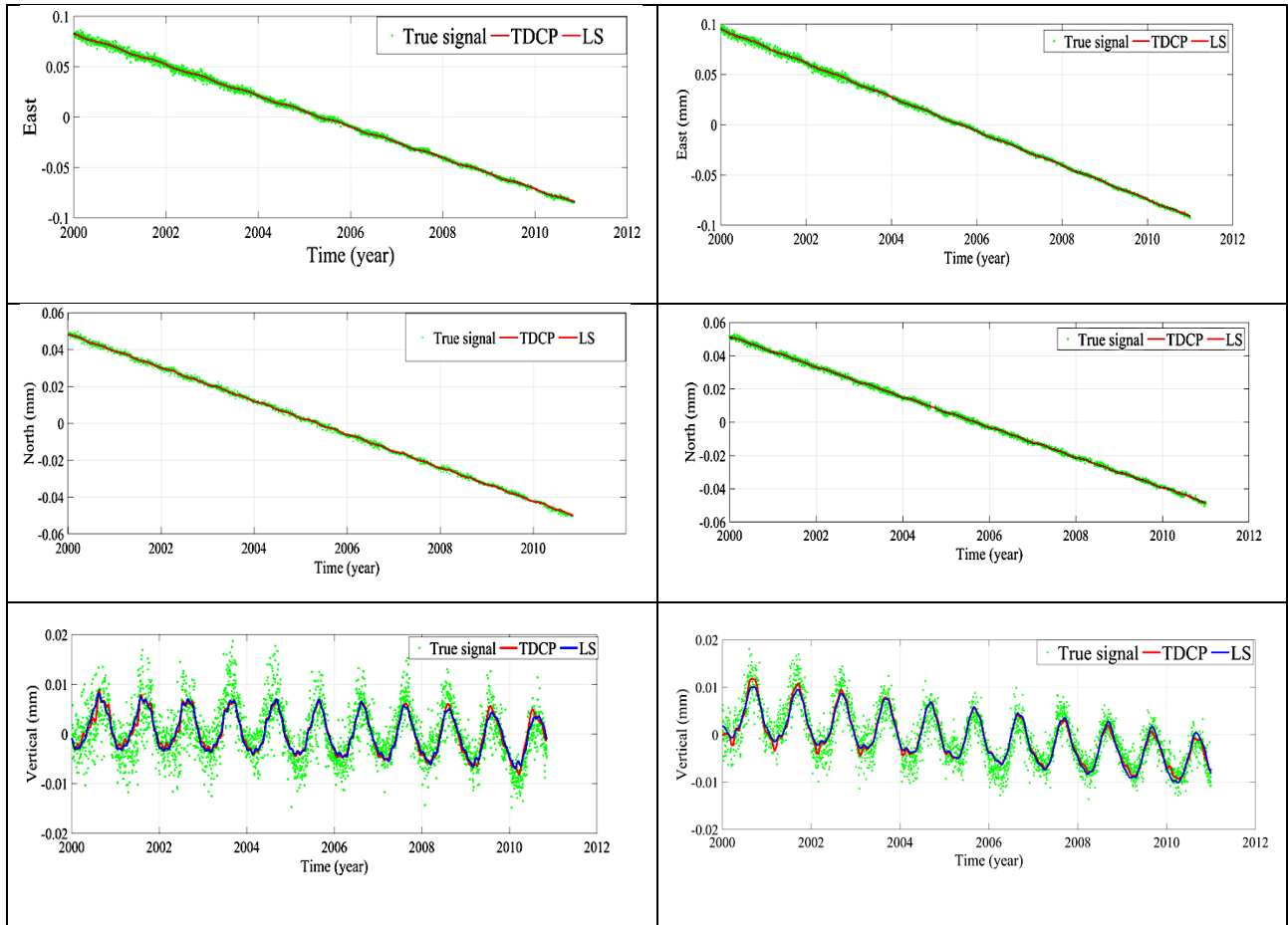


Figure 2. Comparisons of fitting two methods in three components of ALAM station (left panel) and ELKO station (right panel) of selected permanent stations.

Table 1 shows the list of RMS values of the residues from the two models after removing the systematic effects of coordinate components of the nineteen selected stations. Also, the RMS values of the TDPC model are lower than those of the LS method, which is especially noticeable in the vertical component. Moreover, in order to validate the results of real data set using modeling of two models, we simulated the 90 time series of GPS using the periods of the annual and semi-annual periodic signal, and  $350/n$  of significant periodic patterns with periods of 350 days and its fractions  $350/n$ ,  $n = 2, \dots, 8$ , and different combinations of white noise and flicker noise.

Figure 3 illustrates comparing RMS values of the residuals (meters) for 90 simulated time series for two methods using boxplots. That is an alternative method for graphically depicting groups of numerical data through their quartiles. Box plots may also have lines extending from the boxes (whiskers), indicating variability outside the upper

and box and whisker diagram. Outliers are plotted as individual points. The spacings between the different box parts indicate the degree of dispersion and skewness in the data and show outliers. According to Figure 3, in comparison between the RMS of residuals of two models, the results show that the proposed model is superior to LS in its ability to capture signals with modulated amplitudes and phases.

### 5. Conclusion

The main objective of our study is to try to address the problem in an alternative way to extract the modulated periodic cycles from the original GPS time series. Periodic signals in the GPS position time series are conventionally modeled using constant amplitudes and phase lag. However, the amplitude of these signals varies slightly over time. This study shows that the change in amplitude of periodic signals

Table 1. Compare RMS values of the residuals (meters) for modeling of time series of 19 stations in the Western United States were selected from the 2000 and 2010 years.

Site code	Components	RMS Values	
<b>ALAM</b>	Components North East Vertical	LS	
		$7.4075 \times 10^{-4}$	TDPC
		0.0015	
		0.0034	
<b>CAST</b>	North	$7.4416 \times 10^{-4}$	$7.3413 \times 10^{-4}$
	East	0.0014	0.0014
	Vertical	0.0027	0.0033
<b>DYER</b>	North	$7.7047 \times 10^{-4}$	$7.2022 \times 10^{-4}$
	East	0.0014	0.0014
	Vertical	0.0032	0.0026
<b>ELKO</b>	North	$6.9451 \times 10^{-4}$	$7.6493 \times 10^{-4}$
	East	0.0013	0.0014
	Vertical	0.0025	0.0032
<b>FERN</b>	North	$7.7493 \times 10^{-4}$	$6.8401 \times 10^{-4}$
	East	0.0013	0.0013
	Vertical	0.0031	0.0024
<b>FOOT</b>	North	$6.9906 \times 10^{-4}$	$7.5635 \times 10^{-4}$
	East	0.0013	0.0013
	Vertical	0.0027	0.0031
<b>GABB</b>	North	$6.5024 \times 10^{-4}$	$6.9001 \times 10^{-4}$
	East	0.0013	0.0013
	Vertical	0.0026	0.0027
<b>HEBE</b>	North	$9.1626 \times 10^{-4}$	$6.4766 \times 10^{-4}$
	East	0.0018	0.0013
	Vertical	0.0040	0.0025
<b>SHIN</b>	North	$8.5178 \times 10^{-4}$	$9.0799 \times 10^{-4}$
	East	0.0016	0.0017
	Vertical	0.0033	0.0039
<b>AHID</b>	North	$7.6909 \times 10^{-4}$	$8.3848 \times 10^{-4}$
	East	0.0015	0.0016
	Vertical	0.0034	0.0032
<b>ECHO</b>	North	$6.8005 \times 10^{-4}$	$7.4863 \times 10^{-4}$
	East	0.0014	0.0015
	Vertical	0.0026	0.0033
<b>FRED</b>	North	$7.1423 \times 10^{-4}$	$6.7192 \times 10^{-4}$
	East	0.0012	0.0014
	Vertical	0.0030	0.0026
<b>GARL</b>	North	$9.0124 \times 10^{-4}$	$7.0002 \times 10^{-4}$
	East	0.0017	0.0012
	Vertical	0.0043	0.0030
<b>JOHN</b>	North	$9.1080 \times 10^{-4}$	$8.8983 \times 10^{-4}$
	East	0.0015	0.0016
	Vertical	0.0032	0.0043
<b>MONI</b>	North	$7.8478 \times 10^{-4}$	$9.0257 \times 10^{-4}$
	East	0.0014	0.0015
	Vertical	0.0029	0.0032
<b>RAIL</b>	North	$8.0970 \times 10^{-4}$	$7.8093 \times 10^{-4}$
	East	0.0014	0.0014
	Vertical	0.0030	0.0029
<b>RUBY</b>	North	$8.0201 \times 10^{-4}$	$8.0620 \times 10^{-4}$
	East	0.0014	0.0014
	Vertical	0.0029	0.0030
<b>CORV</b>	North	0.0013	$7.9331 \times 10^{-4}$
	East	0.0014	0.0014
	Vertical	0.0033	0.0029
<b>REDM</b>	North	$8.5912 \times 10^{-4}$	0.0013
	East	0.0013	0.0014
	Vertical	0.0029	0.0032

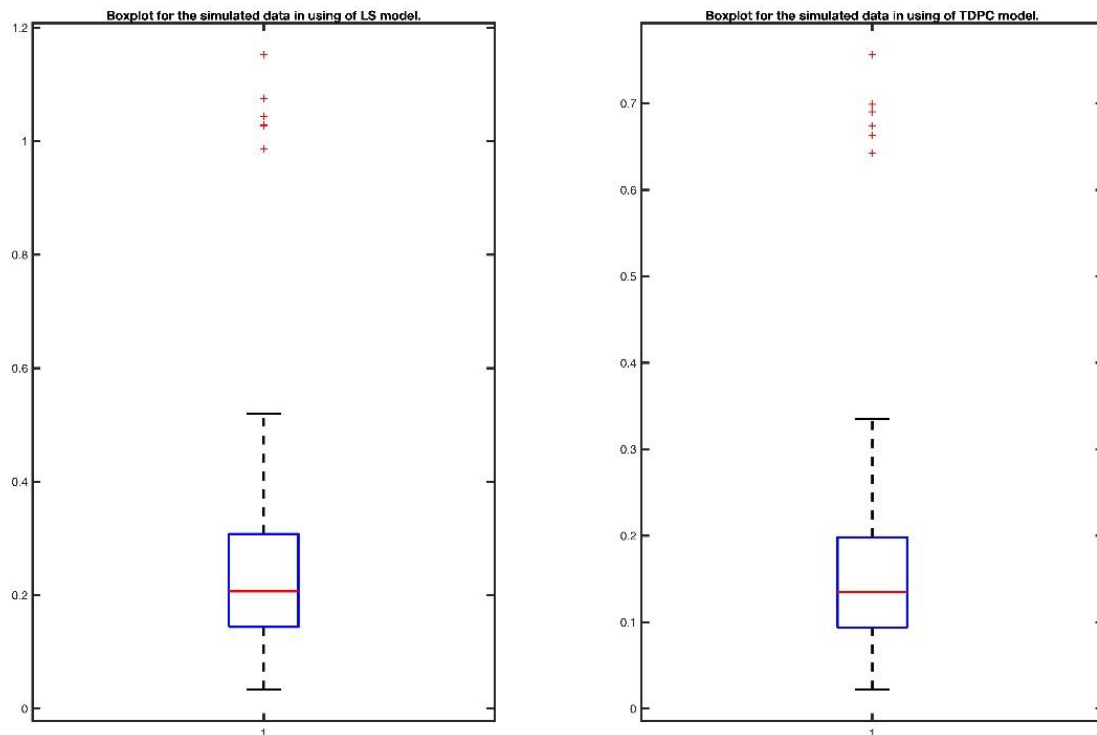


Figure 3. Compare RMS values of the residuals (meters) for 90 simulated time series for two methods using boxplots. The noise of time series were different combinations of white noise and flicker noise.

can be modeled using time varying harmonic coefficients and by differencing observation equations to eliminate autoregressive disturbances. Using the real and simulated GPS data analysis, we demonstrate that the proposed model can extract amplitude varying periodic variabilities from GPS coordinate time series.

### References

Amiri- Simkooei, A.R., Tiberius, C.C. and Teunissen, P.J., 2007. Assessment of noise in GPS coordinate time series: methodology and results. *Journal of Geophysical Research: Solid Earth*, 112 (B7).

Beavan, J., 2005. Noise properties of continuous GPS data from concrete pillar geodetic monuments in New Zealand and comparison with data from US deep drilled braced monuments. *Journal of Geophysical Research: Solid Earth*, 110 (B8).

Blewitt, G. and Lavallée, D., 2002. Effect of annual signals on geodetic velocity. *Journal of Geophysical Research: Solid Earth*, 107 (B7), pp.ETG-9.

Blewitt, G., Lavallée, D., Clarke, P. and Nurutdinov, K., 2001. A new global mode of Earth deformation: Seasonal cycle detected. *Science*, 294 (5550), pp.2342-2345.

Bogusz, J. and Kontny, B., 2011. Estimation of sub-diurnal noise level in GPS time series. *Acta Geodynamica et Geomaterialia*, 8(3), p.163.

Chen, Q., van Dam, T., Sneeuw, N., Collilieux, X., Weigelt, M. and Rebischung, P., 2013. Singular spectrum analysis for modeling seasonal signals from GPS time series. *Journal of Geodynamics*, 72, pp.25-35.

Davis, J.L., Wernicke, B.P. and Tamisiea, M.E., 2012. On seasonal signals in geodetic time series. *Journal of Geophysical Research: Solid Earth*, 117 (B1).

Davis, J.L., Wernicke, B.P., Bisnath, S., Niemi, N.A. and Elósegui, P., 2006. Subcontinental-scale crustal velocity changes along the Pacific North America plate boundary. *Nature*, 441 (7097), pp.1131-1134.

- Davis, J.L., Elósegui, P., Mitrovica, J.X. and Tamisiea, M.E., 2004. Climate- driven deformation of the solid Earth from GRACE and GPS. *Geophysical Research Letters*, 31(24).
- Dong, D., Fang, P., Bock, Y., Cheng, M.K. and Miyazaki, S.I., 2002. Anatomy of apparent seasonal variations from GPS derived site position time series. *Journal of Geophysical Research: Solid Earth*, 107(B4), pp.ETG-9.
- Frey Mueller, J.T., 2009. Seasonal position variations and regional reference frame realization. In *Geodetic Reference Frames* (pp. 191-196). Springer, Berlin, Heidelberg.
- Iz, H.B., 2008. Polar motion modeling, analysis, and prediction with time dependent harmonic coefficients. *Journal of Geodesy*, 82(12), pp.871-881.
- Iz, H.B. and Chen, Y.Q., 1999. VLBI rates with first order autoregressive disturbances. *Journal of Geodynamics*, 28(2-3), pp.131-145.
- Klos, A., Bos, M.S. and Bogusz, J., 2018. Detecting time varying seasonal signal in GPS position time series with different noise levels. *GPS Solutions*, 22(1), pp.1 11.
- Langbein, J., 2004. Noise in two color electronic distance meter measurements revisited. *Journal of Geophysical Research: Solid Earth*, 109(B4).
- Larson, K.M. and van Dam, T., 2000. Measuring post-glacial rebound with GPS and absolute gravity. *Geophysical Research Letters*, 27(23), pp.3925-3928.
- Langbein, J. and Johnson, H., 1997. Correlated errors in geodetic time series: Implications for time dependent deformation. *Journal of Geophysical Research: Solid Earth*, 102(B1), pp.591 603.
- Mao, A., Harrison, C.G. and Dixon, T.H., 1999. Noise in GPS coordinate time series. *Journal of Geophysical Research: Solid Earth*, 104(B2), pp.2797-2816.
- Mandelbrot, B.B. and Van Ness, J.W., 1968. Fractional Brownian motions, fractional noises, and applications. *SIAM Review*, 10(4), pp.422-437.
- Murray, J.R. and Segall, P., 2005. Spatiotemporal evolution of a transient slip event on the San Andreas fault near Parkfield, California. *Journal of Geophysical Research: Solid Earth*, 110(B9).
- Steigenberger, P., Boehm, J. and Tesmer, V., 2009. Comparison of GMF/GPT with VMF1/ECMWF and implications for atmospheric loading. *Journal of Geodesy* 83(10), p.943.
- Tesmer, V., Steigenberger, P., Rothacher, M., Boehm, J. and Meisel, B., 2009. Annual deformation signals from homogeneously reprocessed VLBI and GPS height time series. *Journal of Geodesy*, 83(10), pp.973-988.
- Teferle, F.N., Bingley, R.M., Orliac, E.J., Williams, S.D.P., Woodworth, P.L., McLaughlin, D., Baker, T.F., Shennan, I., Milne, G.A., Bradley, S.L. and Hansen, D.N., 2009. Crustal motions in Great Britain: evidence from continuous GPS, absolute gravity and Holocene sea level data. *Geophysical Journal International* 178(1), pp.23 46.
- Tehranchi, R., Moghtased Azar, K., Safari, A., 2020. A new statistical test based on the WR for detecting offsets in GPS experiment. *Earth and Space Science*, 7, e2019EA000810. <https://doi.org/10.1029/2019EA000810>.
- Tobita, M., 2016. Combined logarithmic and exponential function model for fitting postseismic GNSS time series after 2011 Tohoku-Oki earthquake. *Earth, Planets and Space*, 68(1), pp.1 12.
- Van Dam, T., Wahr, J., Milly, P.C.D., Shmakin, A.B., Blewitt, G., Lavallée, D. and Larson, K.M., 2001. Crustal displacements due to continental water loading. *Geophysical Research Letters*, 28(4), pp.651-654.
- Williams, S.D., Bock, Y., Fang, P., Jamason, P., Nikolaidis, R.M., Prawirodirdjo, L., Miller, M. and Johnson, D.J., 2004. Error analysis of continuous GPS position time series. *Journal of Geophysical Research: Solid Earth* 109(B3).
- Williams, S.D.P., 2003. The effect of coloured noise on the uncertainties of rates estimated from geodetic time series. *Journal of Geodesy*, 76(9 10), pp.483 494.
- Zhang, C.D., Wu, X.P., Hao, J.M., He, H.B. and Zhao, D.M., 2004. ISO2002: an analytical stochastic model of multi difference GPS carrier phase data. *Journal of geodesy*, 78(4 5), pp.263 271.
- Zhang, J., Bock, Y., Johnson, H., Fang, P., Williams, S., Genrich, J., Wdowinski, S. and Behr, J., 1997. Southern California Permanent GPS Geodetic Array: Error analysis of daily position estimates and site velocities. *Journal of geophysical research: solid earth* 102 (B8), pp.18035-18055.